Surface-Modified Zinc Oxide Nanoparticles for Anti-Algal and Anti-Yeast Applications

Ahmed F. Halbus,[a,b] Tommy S. Horozov,[a] Vesselin N. Paunov[a]*

[a] Department of Chemistry and Biochemistry, University of Hull, Cottingham Road, Hull, HU67RX, UK;

[b] Department of Chemistry, College of Science, University of Babylon, Hilla 51001, Iraq

KEYWORDS ZnONPs; antimicrobial nanoparticles; zinc oxide; zinc sulfide; silica; polyelectrolytes; poly (allyl amine) hydrochloride; poly (styrene sulfonate); antimicrobial nanoparticles; S. cerevisiae; C. reinhardtii;

ABSTRACT: We explored the factors and mechanisms of the anti-yeast and anti-algal effect of zinc oxide nanoparticles (ZnONPs) coated with zinc sulfide (ZnS), silica (SiO_2), poly(sodium 4-styrene sulfonate) sodium salt (PSS) and poly(allylamine hydrochloride) (PAH) polyelectrolytes. We examined the activity of various concentrations of surface modified ZnONPs towards microalgae (*C. reinhardtii*) and yeast (*S. cerevisiae*) cells upon irradiation with visible or UV light as well as under dark condition. We investigated the anti-yeast and anti-algal activity of bare ZnONPs upon illumination with UV light compared with that under visible light and in dark conditions to evaluate the impact of the oxidative stress due to the reactive oxygen species (ROS). We also prepared ZnS-coated ZnONPs, SiO_2-coated ZnONPs and combinations of polyelectrolyte (PSS and PAH)-coated ZnONPs and examined their anti-yeast and anti-algal effects. The nanoparticles of anionic surface (ZnONPs/ZnS, ZnONPs/SiO_2 and ZnONPs/PSS) showed much lower anti-algal and anti-yeast activity than the ones with a cationic surface functionality (ZnONPs/PSS/PAH and uncoated ZnONPs). The effect of the ZnONPs surface coating was found to be much stronger than the ROS effect due to illumination with UV light. This indicates that the nanoparticles attachment to the microbial cell wall is much more important for their antimicrobial action than the ROS generation alone. This could be explained by the poor adhesion of ZnONPs/ZnS, ZnONPs/SiO_2 and ZnONPs/PSS to the cells due to electrostatic repulsion. In contrast, the particle-cell electrostatic adhesion in the case of cationic ZnONPs/PSS/PAH and unmodified ZnONPs led to enhanced anti-yeast and anti-algal action. This study brings important insights about the role of the ZnONPs surface coatings on their nanotoxicity and antimicrobial action and could potentially lead to the development better anti-biofouling coatings and anti-yeast formulations.

1. Introduction

ZnO is not generally considered a toxic material, and is accepted as biocompatible.[1] However recent reports point out that it nano-particulate form (ZnONPs) can exhibit certain toxicity effects due to its photocatalytic activity.[2-3] ZnONPs absorb in the UV region[4] which promotes their interactions with molecules in their immediate vicinity. This photocatalytic process can continue long after their activation by UV absorption and has been attributed to the depletion of surface electrons linked to adsorbed negatively charged oxygen derivatives (O_2^{2-}, $O_2^{\bullet-}$) on the ZnONPs surface.[5] Upon activation with UV light in the presence of oxygen, aqueous dispersions of ZnONPs show a phototoxic action due to the formation of reactive oxygen species (ROS) and lead to generation of hydrogen peroxide (H_2O_2), which has an antimicrobial effect.[6] The generated ROS can diffuse into microbial cells and can damage their interior and cell walls, thus inhibiting their growth. The photocatalytic effect underpins the understanding of the antimicrobial action of ZnONPs in medicinal formulations and other nanotech applications. Hence, the enhancement of the antimicrobial activity of ZnONPs has been regarded as a result of the creation of more free radicals, upon activation with UV light.[7-8] Seven *et al*. and other groups have discussed possible reaction mechanism of this effect.[9-14] Nagarajan and Rajagopalan[10] established a link between the photon-initiated process of the photocatalytic particles and their antimicrobial effect.

Sawai *et al*. also associated the cell membranes damage to the peroxidation process of the unsaturated phospholipids due to the photo-catalytically generated H_2O_2 and ROS.[14] Dunford *et al*. [15] explored the effect of ZnO on DNA upon UV irradiation *in vivo*. The antimicrobial effect ZnONPs has been tested against *S. aureus, E. coli* and other bacteria.[16-19] Aruoja *et al*. examined the growth inhibition action of ZnONPs on *Pseudokirchneriella subcapitata*.[20] Heinlaan *et al*. reported a nano-toxic effect of ZnONPs on *Vibrio fischeri, Thamnocephalus platyurus* and *D. magna*.[21] Generally, the toxicity of metal oxide nanoparticles, as well as ZnONPs, is sensitive to the particle morphology, size, their preparation method, the tested microorganisms and other factors.[5,21,22,51,52] In other studies.[23] treated *Eisenia fetida* in soil with various ZnONPs concentrations and reported that a substantial damage can occur above 1.0 g kg^{-1} ZnONPs due to impacting the cellulase activity and the cell DNA. The nanotoxicity of bare ZnONPs on *S. cerevisiae* was examined for up to 24 h. Both bulk ZnO and ZnONPs were reported to have similar toxicity for *S. cerevisiae*. In contrast, other metal oxides nanoparticles like CuONPs produced over 60 times higher toxicity in comparison with bulk CuO. However, bulk TiO_2 and TiO_2NPs are both reported to be non-toxic against *S. cerevisiae* even at very high concentrations.[8, 24]

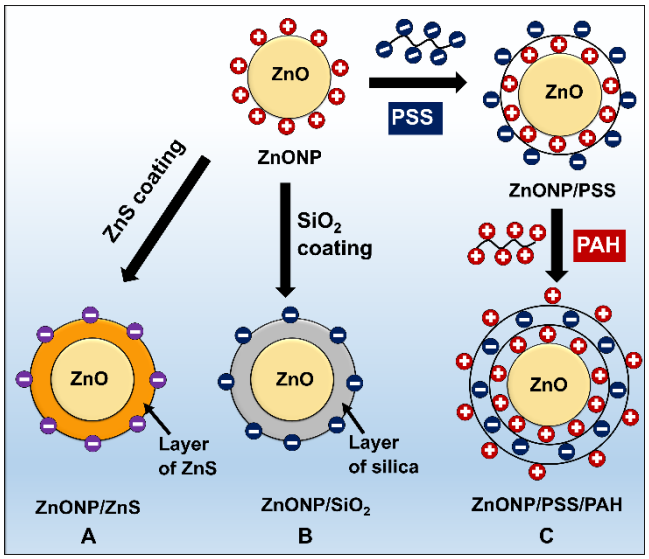

Figure 1. The schematic coating of bare ZnONPs with (A) ZnS, (B) SiO_2 and (C) two consecutive layers of anionic (70 kDa PSS) and cationic (15 kDa PAH) polyelectrolytes in 1 mM NaCl.

In the present work, we study the role of the surface coatings made of zinc sulfide, silica and anionic and cationic polyelectrolytes on the antimicrobial activity of ZnONPs. Two different types of microbial cells, *S.cerevisiae* and *C. reinhardtii*, were used as representative microorganisms to examine the anti-yeast and anti-algal effect of the surface modified ZnONPs. We studied the link between anti-yeast the anti-algal effect of varying the particle size, surface charge, on their ability to attach to the microbial cells. The nanoparticles size is crucial for their potential antimicrobial activity, as smaller nanoparticles are perceived to have larger overall surface area in suspension and higher portability to penetrate through biological membranes.[25] The ZnONPs surface charge determines their ability to electrostatically attach to the biological membranes. We explore the nanoparticle potential for internalization into *C. reinhardtii* and *S.cerevisiae*. This was done after removal of the growth media whose components may adsorb and alter the original particle surface charge. The tested systems are presented on Figure 1. The hypothesis which we are exploring here is that coating of the ZnONPs with an outer layer of a cationic polyelectrolyte may enhance their antimicrobial activity while coating them with an outer layer of ZnS, silica and an anionic polyelectrolyte may decrease their activity due to electrostatic repulsion from the negatively charged microbial cell walls.

2. Experimental Section

2.1. Materials

Zinc nitrate (99%, Sigma Aldrich, UK), potassium hydroxide (85%, Sigma Aldrich, UK) and fluorescein diacetate (FDA, 98%, Fluka, UK) were used as supplied. Ammonia (35 wt% aqueous solution), sodium sulfide (60 wt% aqueous solution), sodium poly(sodium 4-styrene sulfonate) (PSS, average M.W. 70 kDa), poly(allylamine hydrochloride) (PAH, average M.W. 15 kDa) and tetraethylorthosilicate (TEOS), were sourced from Sigma Aldrich, UK. In all experiments we used deionized water produced by Milli-Q reverse osmosis system (from Millipore, UK). *S. cerevisiae* was sourced from Sigma-Aldrich, UK and was cultured using the following protocol. 10 mg of lyophilized *S. cerevisiae* was suspended in 10 mL pre-autoclaved deionized water. Then, 1 mL aliquot the *S. cerevisiae* suspension was mixed with 100 mL pre-autoclaved culture media (YPD: *S. cerevisiae* extract, peptone and dextrose) and incubated at 30 ^{o}C for 2 days.[26] *Chlamydomonas reinhardtii* (cc-124 strain) was received as a gift from Prof Flickinger's group at North Carolina State University, Raleigh, USA. *C. reinhardtii* was cultured in Tris-Acetate-Phosphate (TAP) medium (pH 7) at 30 °C. The TAP media consisted of the following salts ($MgSO_4.7H_2O$, NH_4Cl and $CaCl_2.2H_2O$), phosphate buffer saline (PBS) and a solution of Hutner's trace elements (EDTA disodium salt, H_3BO_3, $ZnSO_4.7H_2O$, $MnCl_2.4H_2O$, $CuSO_4.5H_2O$, $CoCl_2.6H_2O$, $FeSO_4.7H_2O$, $(NH_4)_6Mo_7O_{24}.4H_2O$), all sourced from Sigma-Aldrich, UK. *C. reinhardtii* was cultured in TAP media for 72 h under constant stirring with a magnetic stirrer while being illuminated with a luminescent lamp of a white light intensity of 60 W m^{-2}.

2.2. Synthesis of ZnONPs

Direct precipitation method was used for the synthesis of ZnONPs from $Zn(NO_3)_2$ as a precursor and KOH as a precipitating agent. 0.2 M aqueous solution of $Zn(NO_3)_2$ and 0.4 M solution of KOH were prepared and in the first step, 0.4 M KOH solution was added dropwise to the 0.2 M $Zn(NO_3)_2$ solution while stirring at 25 °C which produced a white dispersion. The white sediment was collectted by centrifugation at 5000 g for 30 min and washed trice with deionized water, ethanol and dried in a vacuum oven (Gallenkamp) for 3 h at 60 °C. [27] In order to produce ZnO of various nano-crystallite sizes, the bulk ZnO was annealed for 3 h at several different temperatures from 100 °C to 600 °C. The crystallite sizes of the synthesized ZnO in solid state were characterized via TEM, XRD, BET, SEM and FTIR. The ZnONPs were formed by sonicating a sample of ZnO in water for 15 min at pH 7.37 by using a digital sonicator (Branson Ltd) at 40% power amplitude set at 2.0 s long ON/OFF pulse intervals. The produced ZnONPs were characterized using a Zetasizer Nano ZL (Malvern, UK). The effect of pH on the particle size and the zeta potential distributions of ZnONPs was examined by adjusted pH from 5 to 12 by dropwise addition of 0.1 M NaOH or 0.1 M HCl solutions.

2.3. Preparation of ZnONPs/ZnS core shell nanoparticles

ZnONPs were surface-modified with a layer of zinc sulfide (ZnS) by the following procedure. 0.05 g of the ZnONPs was dispersed in 50 mL deionized water by sonication for 10 min. After adjusting the pH to 7.37 using 0.1 M NaOH or 0.1 M HCl, a solution of 0.1 M sodium sulfide (Na_2S) was added dropwise to a ZnONPs suspension with constant stirring at 60 ^{o}C for 2 h. The core-shell ZnONPs/ZnS particle were washed trice with water by centrifugation and dried at 70 ^{o}C.[28] The ZnONPs/ZnS samples were characterized by measuring their zeta potential and particle size distribution.

2.4. Preparation of ZnONPs/SiO_2

ZnONPs were coated with a silica layer using 0.05 g ZnONPs dispersed in 50 mL deionized water by sonication for 10 min. Silica shells were produced on the ZnONPs by the Stöber

method, using tetraethoxysilane (TEOS) hydrolyzed using excess of ammonia (NH_4OH, 35 wt%) as a catalyst.[29-31]

1 mL of the NH_4OH solution was added to the ZnONPs dispersion with stirring for 5 min to ensure complete mixing at room temperature. Further, 0.25 mL of TEOS was dissolved in 1:1 ethanol-to-water mixture. Then, the solution of TEOS was added dropwise to the ZnONP dispersion and the reaction proceeded at room temperature for 24 h under continuous stirring with a magnetic stirrer. After that, the ZnONPs/SiO_2 core-shell nanoparticles were collected by centrifugation, and washed trice with absolute ethanol and deionized water to remove any unreacted TEOS and ammonia. The particle zeta potential and size distributions were characterized by Zetasizer Nano ZL.

2.5. Preparation of Polyelectrolyte-Coated ZnONPs

Polyelectrolyte–coated ZnONPs were prepared using ZnONPs synthesized after annealing of ZnO at 100 ºC. An aliquot of 50 mL of 1000 µg mL^{-1} ZnONPs dispersion was added dropwise to an equal volume of 50 mg mL^{-1} PSS solution in 1 mM NaCl. After homogenizing for 1 h on orbital shaker, the samples were washed trice with water by centrifugation at 10000 g for 1 h to remove the excess of PSS. The ZnONPs/PSS particles were re-suspended in 50 mL water[22] and characterized by measuring their particle size and zeta potential distributions. To prepare PAH-coated ZnONPs from this batch, the PSS-coated ZnONPs suspension was added dropwise into 50 mL of 50 mg mL^{-1} PAH solution in 1 mM NaCl. The dispersion was shaken for 20 min and centrifuged trice at 10000 g for 1 h to produce ZnONPs/PSS/PAH (see Figure S1 (ESI)). The impact of utilizing different techniques to add ZnONPs to PSS was investigated, including a dropwise addition with ultra-sonication, direct addition and drop by drop (see Figure S2A and S2B, ESI). The data in Figure S4 (ESI) show that the zeta potential of the ZnONPs/PSS nanoparticles is fairly constant over 24 h after preparation, i.e. the PSS coating is stable.

2.6. ZnONPs Characterization and SEM/TEM Imaging

Thermogravimetric analysis (TGA) of ZnONPs was performed under nitrogen atmosphere using a Mettler Toledo TGA/DSC instrument. The ZnO crystallite size at different temperatures was measured by using Siemens D5000 X-Ray Diffractometer at 0.15418 nm wavelength. The morphology of ZnONPs attached on bacteria was examined by using JEOL JSM-6480 LV SEM instrument. The effect of the particle size and the morphology of bare and modified ZnONPs on their attachment on the microbial cells wall was imaged using JEM 2011 (JEOL, Japan) Transmission Electron Microscopy (TEM).

2.7. Cytotoxicity Assay of ZnONPs coated with ZnS, SiO_2 and Polyelectrolytes on *S. cerevisiae*

The effect of bare and surface modified ZnONPs on *S. cerevisiae* cell viability was tested after separating the cells from their culture media. 30 mL of *S. cerevisiae* dispersion was washed trice by centrifugation with deionized water then re-suspended in 30 mL water. An aliquot of 5 mL *S. cerevisiae* suspension was mixed with 5 mL of ZnONPs suspension at different nanoparticle concentrations. After treatment, 1 mL aliquot of each sample of *S. cerevisiae* was washed with water to discard the excess of ZnONPs by centrifugation for 4 min at 3500 g. The cells were re-dispersed in deionized water (1 mL), and mixed with 2 drops of acetone solution of 1 mM FDA and incubated for 15 min. After that, the samples were washed 3 times with deionized water by centrifugation at 3500 g for 4 min. The cell viability was tested by using a cell counter (Nexcelom Auto X4 Fluorescence Cellometer). The same protocol was used to test the *S. cerevisiae* cell viability after treatment with ZnONPs coated with ZnS, SiO_2 and combination of polyelectrolytes (PSS and PAH).

2.8. Anti-algal Activity of ZnONPs Coated with ZnS, SiO_2 and Polyelectrolytes on *C. reinhardtii*

The *C. reinhardtii* cell viability was examined using FDA live/dead assay similarly to the protocol described in section 2.7. The same approach was used to test the effect of ZnONPs coated with SiO_2, ZnS, PSS and PAH on the viability of *C. reinhardtii*, after incubation with various nanoparticle concentrations for several exposure times.

2.9. SEM and TEM Sample Preparation Protocol for *C. reinhardtii* and *S. cerevisiae* after Exposure to Bare- and ZnS-, SiO_2- and Polyelectrolyte-Coated ZnONPs.

After incubation with the bare- or ZnS-coated, silica-coated and polyelectrolyte-coated ZnONPs at various particle concentrations, the *C. reinhardtii* and *S. cerevisiae* cell samples were washed trice by centrifugation. Further, they were fixed with 2.5 wt% glutaraldehyde solution in 0.1M cacodylate buffer at pH 7.2 and 25 °C for 2 h. These samples were treated additionally for 1 h with 1 wt% osmium tetroxide and the dehydrated in a series of ethanol-water mixtures of increasing ethanol percentage from 50 vol% up to 100 vol% and completed with critical point drying. The fixed cells were also used for TEM imaging after further treatment with 2.5 wt% uranyl acetate for 1 h and washed with ethanol-water mixtures of increasing percentage of ethanol. Following dehydration by critical point drying, the microbial cell samples were prepared for TEM imaging by embedding in epoxy/Araldite resin at 60 ºC for 2 days, cured at 25 ºC for 2 days and sectioned with an ultra-microtome.[32-33] Algae and yeast samples before and after treatment with the modified ZnONPs were imaged by SEM (JEOL JSM-6480 LV) and TEM (EM 2011, JEOL, Japan).

3. Results and Discussion

3.1. Preparation and Characterization of ZnONPs

Figure S5A (ESI) shows the UV–Vis spectra of the produced ZnO. The absorption peak corresponds to the ZnO sample treated by annealing at 100 ºC showing a strong absorbance at a wavelength of 378 nm. This is attributed to the intrinsic band gap absorption of ZnO because of the electrons moving from the valence band (VB) to the conduction band (CB).[34] The band gap energy (E_g) of ZnO was calculated using the equation $E_g = hc/\lambda$, where c is the speed of light (3.0×10^8 m/s); h is the Planks constant, 6.626×10^{-34} J s, and λ is the wavelength (m).[35-36] The band-gap energy was found to be 3.27 eV. The mean zeta potential and hydrodynamic diameter of ZnONPs in water at pH 7.37 were meaured by dynamic light scattering (DLS) of dispersions prepared by dispersing 0.2 mg of ZnO sample in 10 mL of deionized water by ultrasonication. The average particle diameter of ZnONPs was determined to be 82 ± 10 nm with an average zeta potential of +32 ± 5 mV (see Figures S3A and S3B).

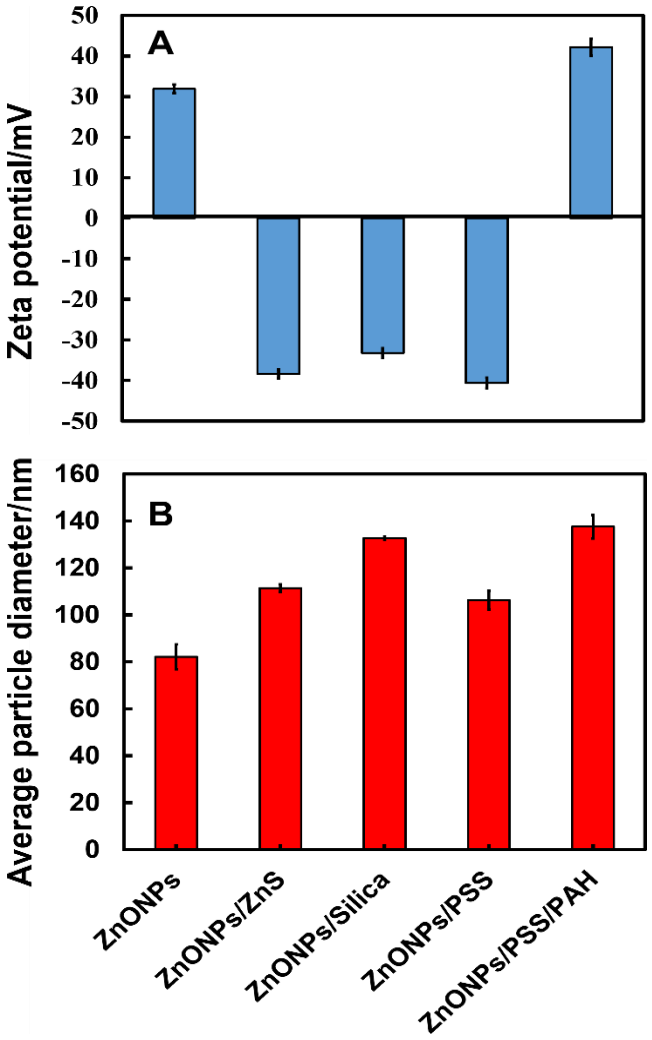

Figure 2. (A) The average zeta potential and (B) the average particle hydrodynamic diameter of bare and coated ZnONPs for different coatings of ZnS, SiO_2, an anionic polyelectrolyte, PSS, and combined PSS coating with an outer layer of a cationic polyelectrolyte PAH dispersed in 1 mM NaCl (error bar represents standard deviation derived from three DLS size distribution measurements).

Surface area measurements of ZnONPs produced from ZnO at various calcination temperatures were carried out by nitrogen adsorption at 77K utilising the BET technique as shown in Figure S3C. Note that the ZnO surface area decreased as the calcination temperature increased from 29 $m^2 g^{-1}$ for 82 ± 10 nm ZnONPs at 100 °C to 7 $m^2 g^{-1}$ for 265 ± 8 nm at 600 °C, in agreement with a previous studies.[37] The particle size and zeta potential of the non-coated ZnONPs were measured in the pH range 5 – 12, as presented in Figure S3D. The produced non-coated ZnONPs had an isoelectric point of around 10.1, i.e. they were cationic particles at neutral pH. As shown in Figure S3D, the particle size increases while the zeta potential decreases upon increasing the pH. TGA carried out in the range between 50 °C and 1000 °C, as shown in Figure S5B (ESI), indicated that the weight loss occurs in two stages upon increasing the temperature. The first weight loss appears in the range of 50 °C to approximately 190 °C because of the removal of absorbed surface water from the particle sample. The second stage is from 190 °C to 350 °C with no further weight loss, indicating the loss of OH groups due to the dehydration. The TGA curve confirms that the precursor can be totally decomposed to ZnO after calcining at approximately 350 °C as also reported by other authors.[38] Figure S6A shows that the hydrodynamic diameter of the resulting ZnONPs increases with increasing annealing temperatures of the ZnO. Thus, it was found that ZnONPs with the same crystallite type but various particle size in aqueous dispersion could be obtained by changing the annealing temperature, also in agreement with a previous work.[40-42] These results may be explained with the fact that at a higher annealing temperature, an agglomeration of ZnO crystallites occurs and hence the ZnONPs particle size increased. The zeta potential was measured for each annealed sample of ZnONPs. Figure S6B shows that for ZnO produced by annealing at 100 °C, the zeta potential of the resulting ZnONPs was +32 ± 5 mV which gives a highly stable dispersion, while for the sample produced by annealing at 600 °C the zeta potential was +15 ± 3 mV. EDX analysis was carried out on the synthesized ZnONPs to verify the elemental composition. Figure S7 (ESI) shows the XRD patterns of the ZnONPs sample obtained from the annealing of ZnO at various temperatures (100 - 600°C) in a muffle furnace to find out the impact of temperature on the ZnO crystallite size. The characteristic peaks for the ZnO sample were in agreement with similar results previously reported in the literature.[39] In the XRD pattern, no peaks related to impurity were identified, confirming that the synthesised product is of high purity. The results showed that there is a change in the crystallinity of the ZnONPs by increasing the annealing temperatures from 100 to 600°C as shown in Figure S7 (ESI). The average size of the ZnO crystallites was estimated using the Scherer equation. The EDX data in Figure S8 (ESI) confirmed the presence of zinc and oxygen signals in the zinc oxide nanoparticle sample. The elemental analysis of the sample gave 79% of zinc and 20% of oxygen which confirmed that the formed ZnO is in a highly purified form with molar ratio of Zn:O of 1:1 and likewise was in agreement with previous work.[43-44] Figure S6C, S6D and S6E shows TEM images of ZnONPs resulted from the annealing of ZnO at 100 °C, 500 °C and 600 °C for 3 h. TEM images in Figure S6 shows that the particle size is increasing with increasing of the annealing temperatures. For the ZnO sample annealed at 100°C, it was found that the average crystallite size is 16 ± 5 nm (Figure S6C). For the ZnO samples annealed at 500 °C and 600 °C (Figure S6D and S6E), it was found that the average crystallite sizes were 25 ± 11 nm and 43 ± 16 nm, respectively.

3.2. Preparation of ZnONPs/ZnS, ZnONPs/SiO2 and ZnONPs/PSS and ZnONPs/PSS/PAH

The formation schematics of ZnONPs/ZnS is illustrated in Figure 1A. After dispersing the ZnONPs in deionized water, the solution pH was adjusted to approximately 7.4. A solution of 0.1 M Na_2S was added dropwise to a suspension of ZnONPs causing an accumulation of S^{2-} ions on the surface of the nanoparticles where they interacted with the Zn^{2+} and lead to the formation of a ZnS layer around the bare ZnONPs. The presence of sulfur in the ZnONPs/ZnS was confirmed by EDX analysis as shown in Figure S9 (ESI). The average hydrodynamic diameter and zeta potential of the ZnONPs/ZnS were 112 ± 6 nm and -38 ± 4 mV, respectively, as shown in

Figure S10 and S11 (ESI). ZnONPs were coated with a layer of silica by the Stöber method by hydrolyzing TEOS in the presence of ammonia in ethanol. After this coating step, these core-shell particles, ZnONPs/SiO_2, were re-dispersed in deionized water. Figure 1B shows the schematic diagram of the silica coating of the bare ZnONPs which reversed their surface charge. The presence of a silica layer over the bare ZnONPs was examined further by the TEM, EDX, zeta potential and particle size measurements. The EDX analysis in Figure S12 (ESI) confirmed the presence of Zn, O and Si signals in the ZnONPs/SiO_2 sample. The TEM images show that a layer of silica with thickness approximately 10-15 nm has been formed on the ZnONPs surface (Figure S13A and S13B, ESI). It was found that the average hydrodynamic diameter of the ZnONPs/SiO_2 was approximately 134 ± 8 nm (Figure S14 (ESI)). The zeta potential of the bare ZnONPs was measured to be +32 ± 5 mV at pH 7.37 but after coating with silica, the zeta potential reversed to -33 ± 3 mV for the ZnONPs/SiO_2 (Figure S15 (ESI)). The negative surface charge of the ZnONPs/SiO_2 was attributed to a complete layer of silica with silanol groups (Si–OH) on the particle surface.[45] Figure 1C schematically illustrates the structure of ZnONPs coated with two layers of PSS and PAH (see Figure S16 and S17, ESI). The average zeta potential and hydrodynamic diameter of the ZnONPs after coating with silica, ZnS, PSS and PAH were measured as shown in Figure 2A and 2B. The results, shown in Figure 2A, indicate that the average zeta potential of the bare ZnONPs does change after each coating. The zeta potential changed from positive (+32 ± 5 mV) for the bare ZnONPs to negative values of -41 ± 2 mV for the ZnONPs/PSS, -33 ± 3 mV for the ZnONPs/SiO_2 and -38 ± 2 mV for the ZnONPs/ZnS. All these core-shell particles were anionic at neutral pH. However, upon further coating of the ZnONPs/PSS with PAH, the particles became positively charged ZnONPs/PSS/PAH with a zeta potential of +42 ± 4 mV.

3.3. Anti-algal Activity of ZnONPs/PSS and ZnONPs/PSS/PAH

We studied the anti-algal activity of ZnONPs coated with one (PSS) or two alternating layers of polyelectrolytes (PSS/PAH) towards *C. reinhardtii* cells upon illumination with visible and UV light as well as in dark conditions. In order to examine the role of the outer polyelectrolyte layer and to control the electrostatic interaction of the ZnONPs functionalized with PSS and PAH, we compared their anti-algal effect with the one of the bare ZnONPs. Aqueous suspensions of *C. reinhardtii* cells were incubated with bare and polyelectrolyte-coated ZnONPs at varying particle concentrations in a range of 1 - 250 μg mL^{-1} for different exposure times. A control sample of *C. reinhardtii* was kept at the same conditions without treatment with ZnONPs for the same period of time. The cell viability of *C. reinhardtii* was tested immediately after removing the excess of ZnONPs from the *C. reinhardtii* suspension.

Figure 3 shows the effect of the bare and coated ZnONPs on *C. reinhardtii* cells in dark, visible and UV light conditions at various exposure times for up to 6 h. The data in Figure 3A show that immediately after incubation (~10 min), the cell viability gradually declined for ZnONPs concentrations higher than 1 μg mL^{-1}. From 2 - 6 h of exposure to visible and UV light, the number of viable algal cells was also reduced (Figure 3B and 3C). At low exposure times to visible and UV light, there was an apparent anti-algal impact for ZnONPs concentrations above 10 μg mL^{-1}. After 2 h of exposure, a steep decrease in the algal cells viability was measured for ZnONPs concentrations in the range of 10 - 250 μg mL^{-1}. At 250 μg mL^{-1} ZnONPs after 6 h of exposure, the *C. reinhardtii* cells suffered 100% loss of their viability. Figure 3 shows that the anti-algal activity of ZnONPs on the *C. reinhardtii* under UV light for 6 h is higher than that under visible light and in the dark at the similar other conditions. One possible explanation is that aqueous suspensions of ZnONPs under UV light can create ROS like $O_2^{\bullet-}$ and H_2O_2.[6,24] The produced active radicals can kill or inhibit the algal cells in immediate vicinity. The *C. reinhardtii* cell viability also declined in dark conditions with the increase of the particle concentration. This effect can be explained with the positive particle surface charge leading to a strong electrostatic attraction between the cationic surface of the bare ZnONPs and the anionic surface of the algal cell walls, which because of the surface roughness of the ZnONPs, fractures their cell membranes. Figure S18 and Figure S19 (ESI) show the total chlorophyll content (chlorophyll a and b) versus the ZnONPs concentration after various exposure times up to 6 h under dark, visible light and UV light conditions. The results in Figure S18 and Figure S19 (ESI) confirm that the *C. reinhardtii* suffer a partiall loss of their chlorophyll content in the presence of ZnONPs upon exposure to UV light and also upon illumination with visible light. The algae chlorophyll content also decreased under dark conditions in the presence of ZnONPs.

We found a sharp decrease of the microalgae chlorophyll content upon illumination with visible and UV light above ZnONPs concentration of 1 μg mL^{-1}. Interestingly, this is near the threshold concentration above which the *C. reinhardtii* cells start losing their viability. We also verified that the *C. reinhardtii* cells in the absence of ZnONPs did not lose their viability or chlorophyll content at the same conditions (see Figure S20 (ESI)). These results showed that the ZnONPs have a strong impact on the *C. reinhardtii* viability for 6 h of incubation at particle concentrations above 1 μg mL^{-1} (see Figure S21 (ESI)). Similar conclusions have been reached by other authors[10] showing that the ZnONPs aqueous suspensions at lower particle concentrations did not have a significant antibacterial activity towards *E. coli*, and the presence of Zn^{2+} ions in the media may even act as an additional nutrient for the bacteria. In contrast, at the highest particle concentration range (5 - 100 mM) the ZnO particles are known to be toxic to bacteria.[10,46-47] We also studied the anti-algal activity of ZnONPs coated with two alternating polyelectrolyte layers of PSS and PAH and compared them with the bare ZnONPs, as the adhesion of the later to the cell wall is driven mainly by electrostatic forces. Figure 3D, 3E and 3F show the cytotoxic impact of ZnONPs/PSS on the algal cells in dark conditions, and under visible and UV light, respectively. The data in Figure 3D, 3E and 3F show that presence of ZnONPs/PSS has much lower impact on the *C. reinhardtii* viability in dark, visible and UV light conditions is much lower than that of the bare ZnONPs (c.f. Figure 3A, 3B and 3C).

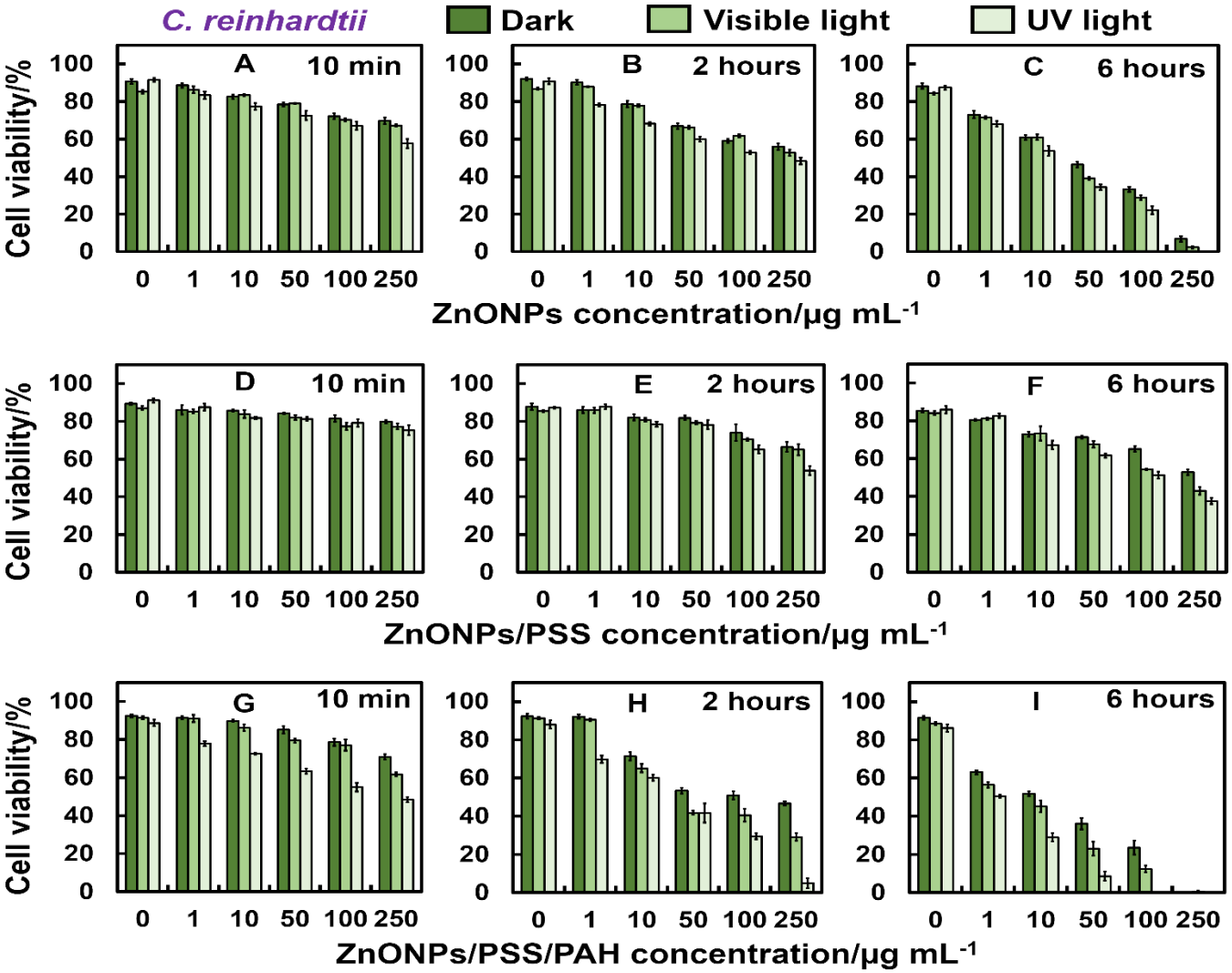

Figure 3. Comparison of the *C. reinhardtii* cell viability at different concentrations of the bare ZnONPs (A−C), and ZnONPs surface functionalized with PSS (D−F), and PAH (G−I) in dark, visible, and UV light conditions at various incubation times (shown). The data are shown as means ± SD of three independent replicates. Statistical analysis of the data is presented in Table S1 (ESI).

After 6 h of incubation at higher particle concentrations of ZnONPs (250 μg mL^{-1}) there was remarkable difference between the *C. reinhardtii* cell viability in dark conditions and under UV light because of the photoactivity of the ZnONPs/PSS. One may conclude that the surface functionalization of the ZnONPs with PSS decreased its anti-algal activity largely because of the electrostatic repulsion of the anionic ZnONPs/PSS from the anionic surface of algal cells. We coated ZnONPs/PSS with an additional layer of PAH which reverses the particles surface charge from negative to positive. The positive surface charge of the ZnONPs/PSS/PAH had a dramatic impact on the viability of *C. reinhardtii.*

The data in Figure 3G, 3H and 3I where an outer layer of PAH was added to the ZnONPs/PSS, showed a significant effect on the *C. reinhardtii* cell viability. At 250 μg mL^{-1} of ZnONPs/PSS/PAH, 100% of the *C. reinhardtii* cells were killed after 6 h of incubation. The tests indicate that these cationic nanoparticles were even more effective than the bare ZnONPs both in dark conditions, and under visible and UV light as shown in Figure 3I. This form of alternating anti-algal activity of the polyelectrolyte-coated ZnONPs appears to be linked to their surface charge and the corresponding electrostatic adhesion to the negatively charged algal cells. These results show that the cationic NPs (the uncoated ZnONPs and ZnONPs/PSS/PAH) have much higher anti-algal activity than their anionic form ZnONPs/PSS.[22]

Figure 4 shows SEM images of *C. reinhardtii* cells after incubation with ZnONPs coated with ZnS, SiO_2, PSS and PAH layers. Figure 4C, 4D and 4E indirectly confirm the lack of nanoparticle accumulation on the algal cells due to the electrostatic repulsion between the anionic nanoparticles, ZnONPs/ZnS, ZnONPs/SiO_2 and ZnONPs/PSS, and the negatively charged cell wall of *C. reinhardtii*. However, Figures 4B and 4F show a significant accumulation of bare ZnONPs and ZnONPs/PSS/PAH on the outer cell walls which yields much higher anti-algal effect.

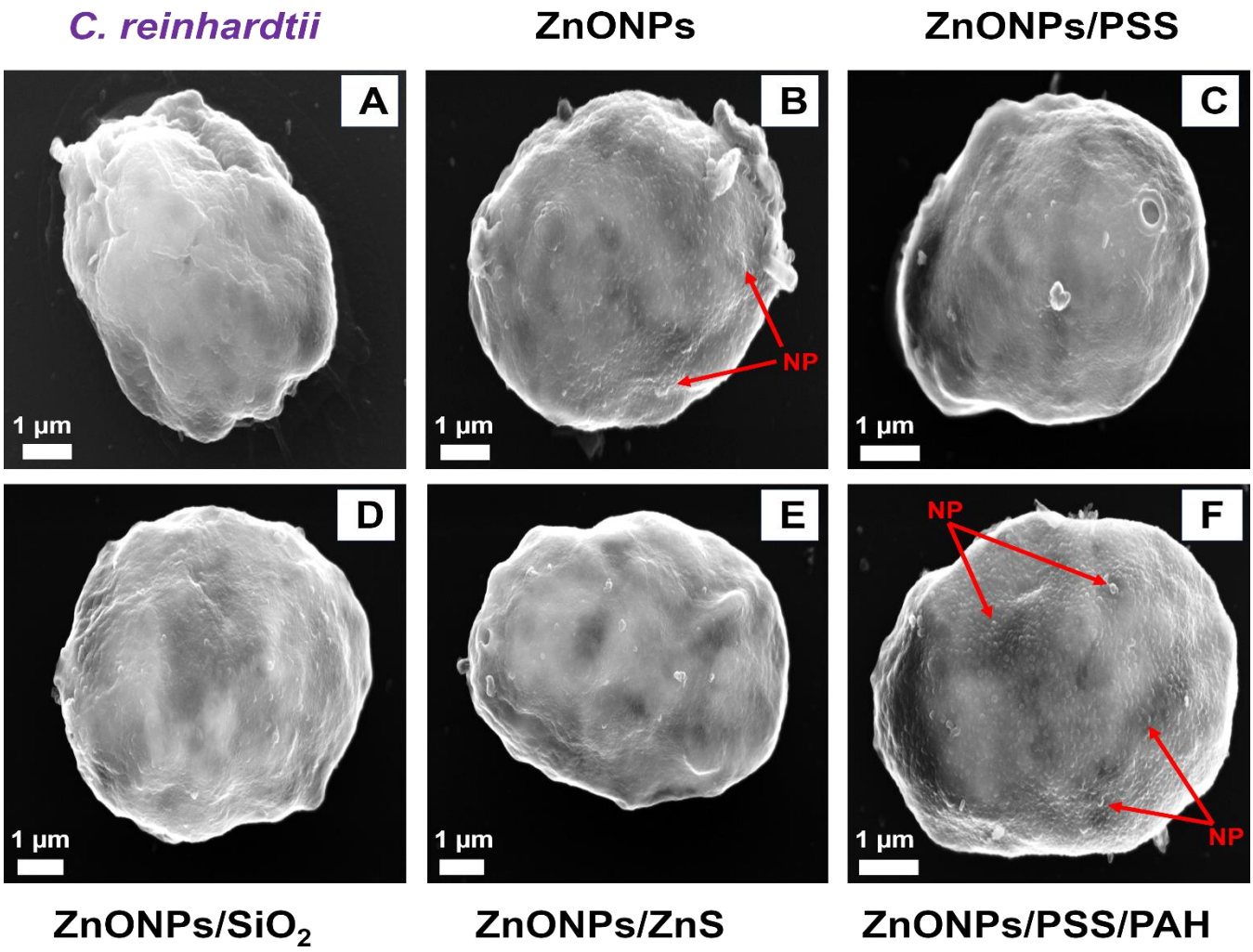

Figure 4. SEM images of samples of *C. reinhardtii* after 6 h of incubation with ZnONPs coated by ZnS, SiO_2, PSS and PAH: (A) an untreated sample, (B) after treatment with bare ZnONPs, (C) ZnONPs/PSS (D) ZnONPs/SiO_2, (E) ZnONPs/ZnS and (F) ZnONPs/PSS/PAH.

3.4. Anti-yeast Activity of Polyelectrolyte-Coated ZnONPs

Toxicity assay of ZnONPs surface functionalized with PSS and PAH was also conducted with *S. cerevisiae* cells after their removal from the culture media. Figure 5A shows that after 10 min of exposure, the percentage of viable *S. cerevisiae* cells declined for ZnONPs concentrations above 10 µg mL^{-1}. After 6 h of incubation (Figure 5C), the *S. cerevisiae* cell viability decreased in the range of concentrations of coated ZnONPs of 10 - 750 µg mL^{-1} under both visible and UV light. However, in dark conditions the cell viability was higher than that that under visible and UV light at the same nanoparticle concentrations. These findings are similar to the results with *C. reinhardtii* at high concentrations of ZnONPs which can also be attributed to the attraction of the surface rough cationic particles with the negatively charged cell membrane leading to their local fracturing. These results also showed that the ZnONPs have a strong impact on *S. cerevisiae* above 250 µg mL^{-1}, both in dark conditions, and under visible and UV light. The cytotoxic impact of the ZnONPs on *C. reinhardtii* upon irradiation with visible and UV light was more pronounced and is detected at much lower concentration of ZnONPs (>10 µg mL^{-1}). The specific cytotoxicity mechanism of ZnONPs under visible and UV light is boosted by the generation of ROS on the ZnONPs surface as they are attached on the cell wall which can potentially produce local oxidation of the components of their cell membrane and its degradation. From the TEM images (Figure 6) we did not see evidence for internalization of ZnONPs through the algal cells walls although some of the generated ROS generated may potentially cause additional DNA damage, disruption of the electron transport chain, and deterioration of cell organelles like chloroplasts, all contributing to the cell death, as recently reported in the literature.[12, 24, 48-50] We found that the ZnONPs have a disruptive impact on the algal cells even in dark condition. The SEM and TEM images of *S. cerevisiae* treated with bare ZnONPs dispersions also showed lack of internalization of ZnONPs. However, the cell walls indicated some disruption due to accumulation of particles on the outer cell wall as seen in Figure 6B and Figure 7B.

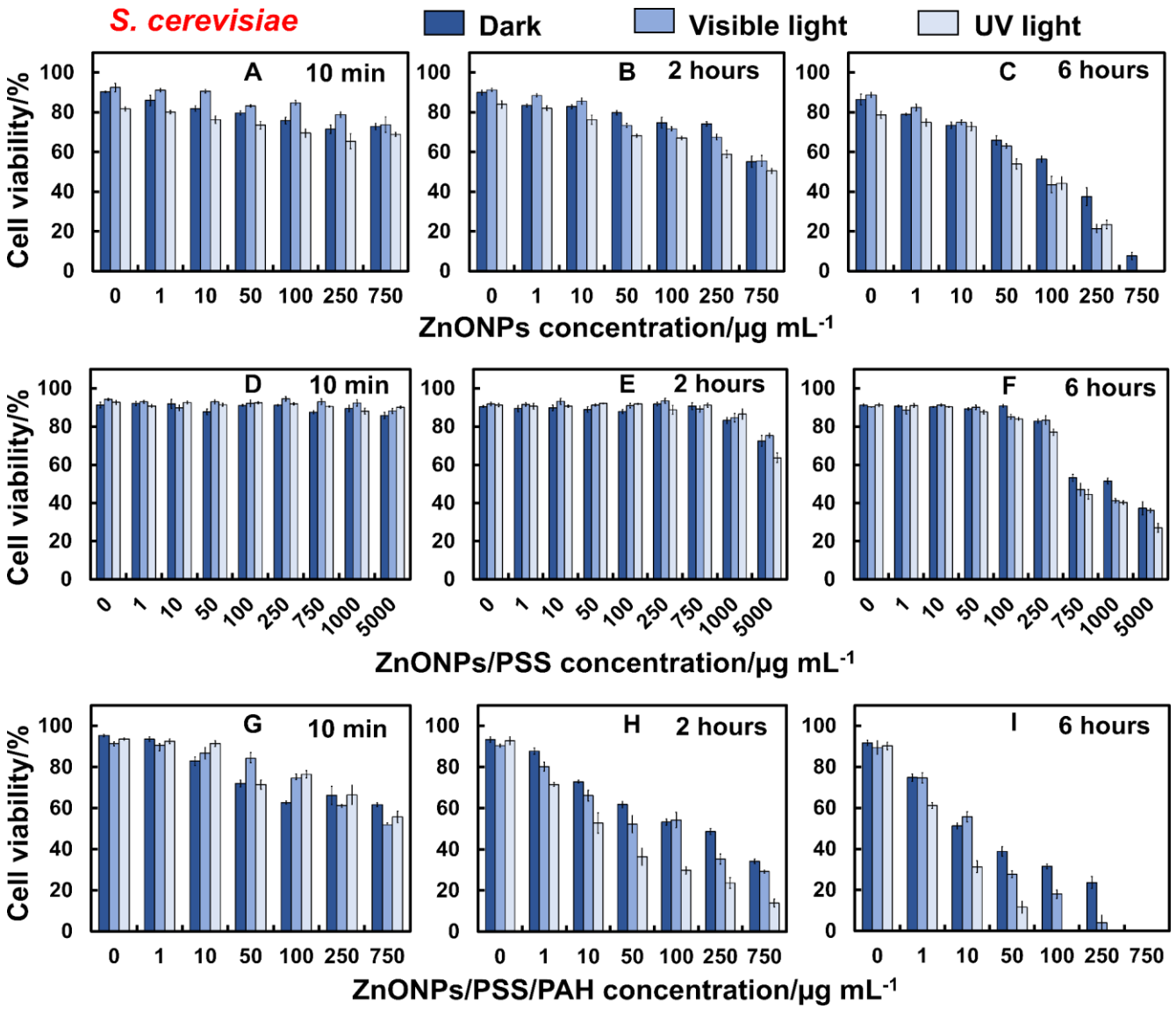

Figure 5. Comparison of the *S. cerevisiae* cell viability versus the concentration of the bare ZnONPs (A - C), and ZnONPs surface functionalized of with PSS (D - F) and PAH (G - I) in dark conditions, and under visible and UV light at various periods of incubation. Error bars indicate standard deviations. The statistical analysis of the data is presented in Table S2 (ESI).

The cell membrane in many of the examined *S. cerevisiae* cells looked compromised. Figure 5D shows that after 10 min of incubation, the *S.cerevisiae* cell viability both in the dark conditions and under visible and UV light was at the same level as the untreated sample. For up to 2 h of incubation of the cells with ZnONP/PSS (Figure 5E), we did not observe toxic effect on the *S. cerevisiae* up to particle concentration of 750 μg mL^{-1}. However, there was a significant impact in the range of ZnONP/PSS concentrations 1000 - 5000 μg mL^{-1} in both dark, visible and UV light conditions. After 6 h of incubation (Figure 5F) with 100 μg mL^{-1} ZnONPs/PSS the samples showed no anti-yeast activity in dark conditions and under visible and UV light. Figures 5G, 5H and 5I show the anti-yeast activity of ZnONPs coated with PSS and PAH at various ZnONPs/PSS/PAH concentrations on viable *S.cerevisiae* cells. Figure 5I indicates that after 6 h of exposure, the ZnONPs/PSS/PAH showed very high anti-yeast activity even at very low particle concentrations in dark conditions, and under visible light and UV light. Stronger anti-yeast activity of the ZnONPs/PSS/PAH was measured on *S.cerevisiae* upon illumination with visible and UV light. Possible explanation of this effect is that under visible and UV light, the *S.cerevisiae* cell walls suffer more damage due to the ROS created in their immediate vicinity which is exacerbated at higher concentrations of the ZnONPs/PSS/PAH and incubation times. In contrast, upon incubation the *S.cerevisiae* cell with the anionic nanoparticles (ZnONPs/PSS), no obvious difference was found between the percentage of viable *S.cerevisiae* cells up to 250 μg mL^{-1} particle concentration for up to 6 h of exposure in dark conditions, and under visible and UV light. These findings were also confirmed by the TEM and SEM images of the treated yeast cells (Figure 6F and Figure 7F).

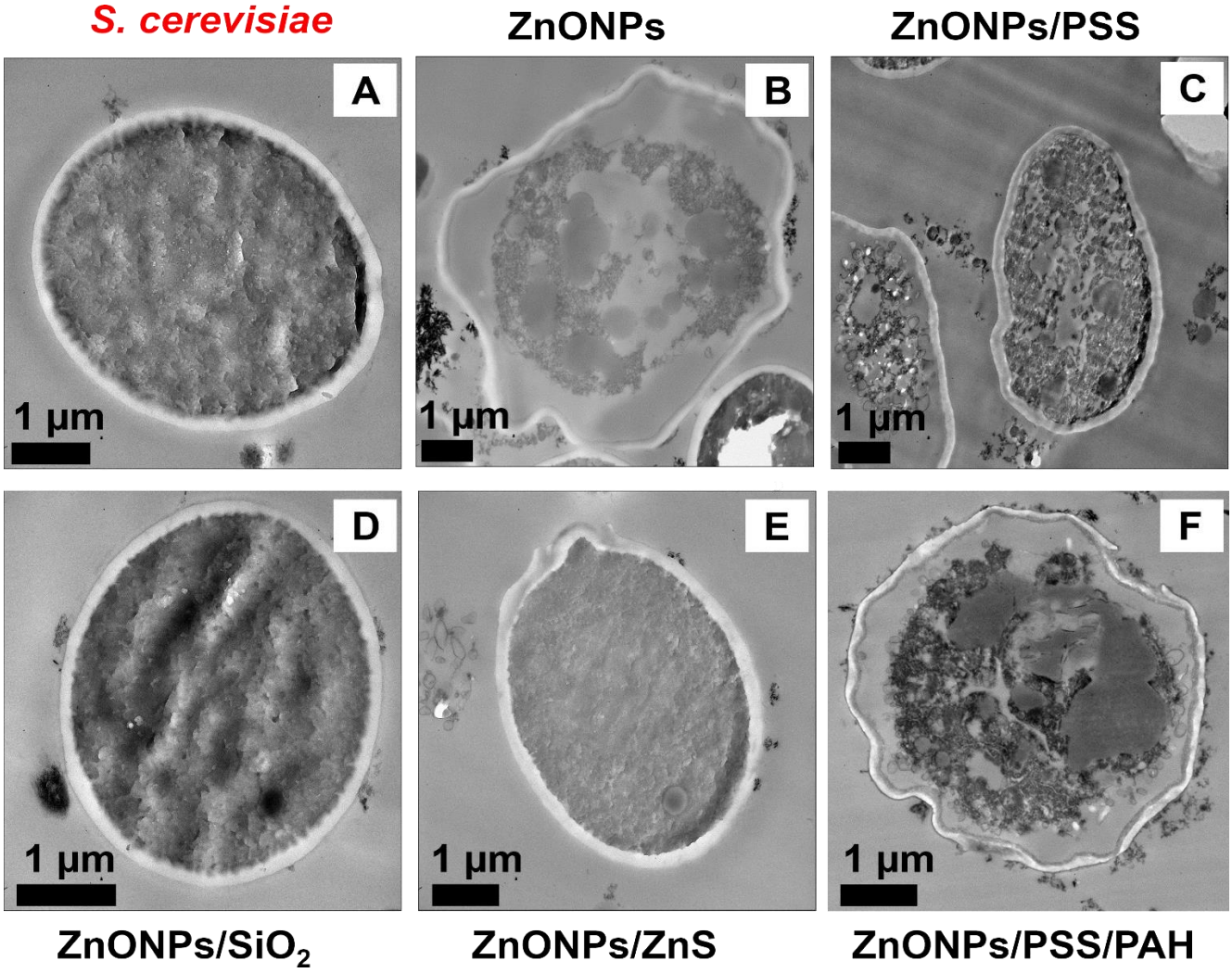

Figure 6. TEM images of *S. cerevisiae* after incubation for 6 h with bare ZnONPs and ZnONPs functionalized with SiO_2, ZnS, PSS and PAH: (A) *S. cerevisiae* before treatment (B) *S. cerevisiae* incubated with 750 µg mL^{-1} bare ZnONPs (C) *S. cerevisiae* incubated with 750 µg mL^{-1} ZnONPs/PSS (D) *S. cerevisiae* treated with 750 µg mL^{-1} ZnONPs/SiO_2 (E) *S. cerevisiae* incubated with 750 µg mL^{-1} ZnONPs/ZnS and (F) *S. cerevisiae* treated with 750 µg mL^{-1} ZnONPs/PSS/PAH. Note the accumulation of (B) ZnONPs and (F) ZnONPs/PSS/PAH on the *S. cerevisiae* cell walls.

The differences between the ZnONPs effect on yeast and microalgae can be explained as *S. cerevisiae* cells have much thicker cell walls (approximately 200 nm) than the *C. reinhardtii* cell walls (<10 nm); the data suggests that it takes a much higher nanoparticle concentration to impact the *S. cerevisiae* cells viability.

3.5. Toxicity Effect of Silica-Coated ZnONPs on *S. cerevisiae* and *C. reinhardtii*

We also investigated the cytotoxic impact of ZnONPs coated with a layer of silica on the *S. cerevisiae* and *C. reinhardtii* cell viability at various exposure time (10 min, 2 h and 6 h). Cells were removed from their culture media and a fixed amount of cells were incubated with dispersed ZnONPs/SiO_2 at different particle concentrations. The results are presented in Figure 8. The cell viability was then measured at various incubation times by using an automatic cell counter by fluorescein diacetate (FDA) live/dead assay. Figures 8A, 8B and 8C show that there was no pronounced toxicity impact of ZnONPs/SiO_2 on the *C. reinhardtii* in all conditions (dark, visible and UV light) after 10 min and 2 h of incubation (Figure 8A and 8B). After 6 h of incubation of *C. reinhardtii* cells (Figure 8C), no pronounced toxicity effect in the *C. reinhardtii* viability was observed up to 50 µg mL^{-1} ZnONPs/SiO_2 but there was a cytotoxic impact of ZnONP/SiO_2 measurable at 100 and 250 µg mL^{-1} ZnONPs/SiO_2 in both of dark, visible and UV light conditions. It was found that the toxicity impact of ZnONPs/SiO_2 on the *C. reinhardtii* at the same conditions is much lower than the one of the bare ZnONPs (see Figure 3A, 3B and 3C). We also confirmed these results by SEM images (Figure 4D) of the treated *C. reinhardtii* cells with ZnONPs/SiO_2 which show no accumulation of particles on the outer cell wall surface.

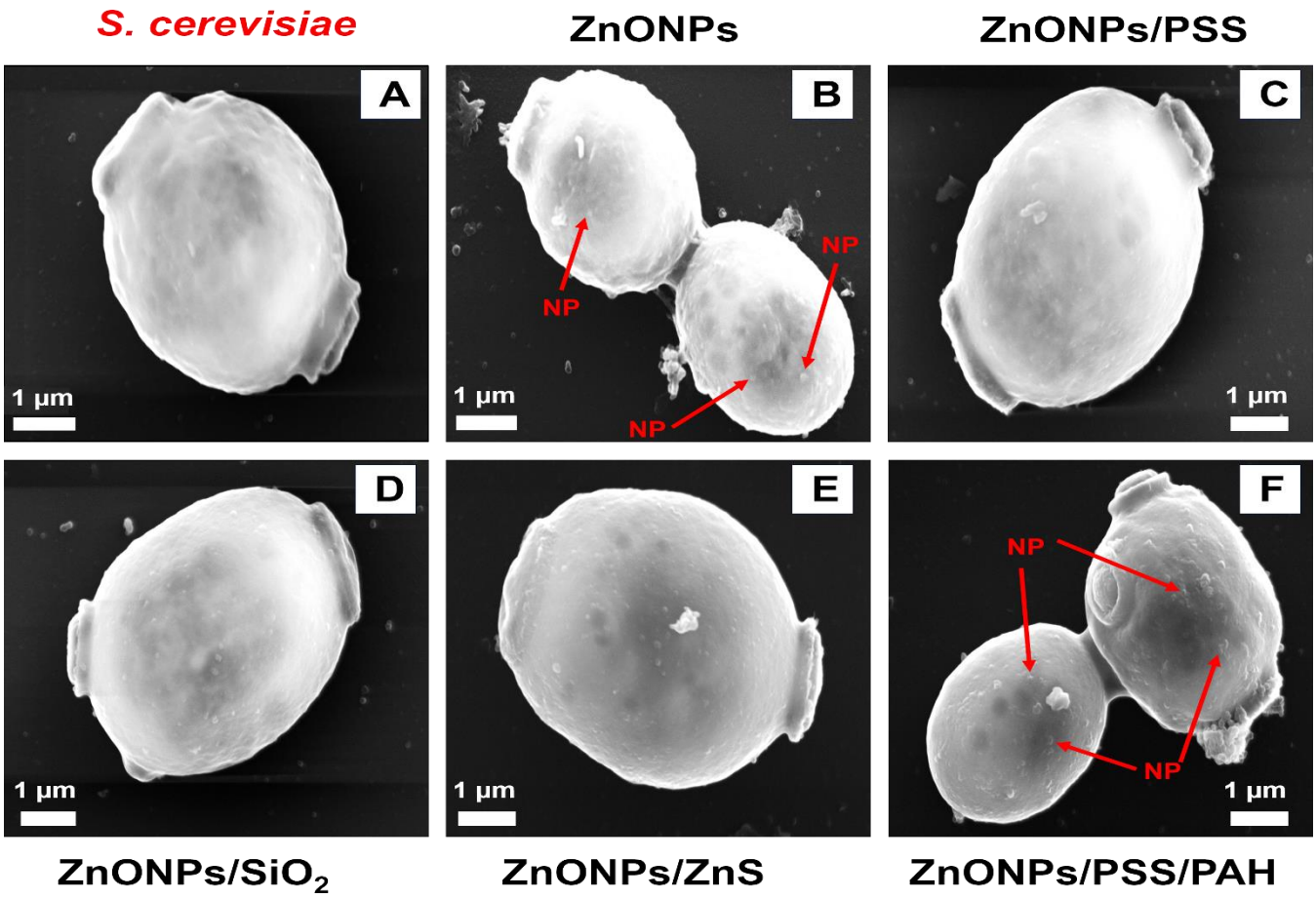

Figure 7. SEM images of *S. cerevisiae* after being incubated for 6 h with 750 µg mL^{-1} bare and surface functionalized of ZnONPs: (A) an untreated *S. cerevisiae* sample without ZnONPs (B) *S.cerevisiae* after being incubated with bare ZnONPs (C) *S. cerevisiae* after being incubated with ZnONPs/PSS (D) *S. cerevisiae* incubated with ZnONPs/SiO$_2$ (E) *S. cerevisiae* after being incubated with ZnONPs/ZnS and (F) *S. cerevisiae* after being incubated with ZnONPs/PSS/PAH.

Figure 8D, 8E and 8F shows the toxicity effect on *S. cerevisiae* cells of different concentrations of ZnONPs/SiO$_2$. Figure 8D and 8E indicate that for 10 min and 2 h of exposure, no significant change in the yeast cell viability was observed even at high ZnONPs/SiO$_2$ concentrations. Likewise, important differences were not seen between the samples under dark conditions or under visible and UV light at the same concentration of ZnONPs/SiO$_2$. Figure 8F shows that after 6 h of incubation, for particle concentrations in the range of 1-100 µg mL^{-1} ZnONPs/SiO$_2$ there was no impact, but at 250 µg mL^{-1} ZnONPs/SiO$_2$ there was a slight decrease in the yeast cell viability in under UV light compared to the one in the dark at the same conditions. The percentage of *S. cerevisiae* viability significantly decreased from 750 to 5000 µg mL^{-1} ZnONPs/SiO$_2$. We discovered that at 5000 µg mL^{-1} ZnONPs/SiO$_2$ under UV light, a significant toxic impact occurred with approximately 20% viability loss in comparison with the control. A very similar impact was observed for ZnONPs/SiO$_2$ with ZnONPs/PSS (see Figure 3 and Figure 5) on the *C. reinhardtii* and *S. cerevisiae* cells which is most likely due to the electrostatic repulsion with the cell wall as both have negatively charged surfaces in aqueous media, which leads to reduced toxicity. Figure 6D and 7D show TEM and SEM images of *S. cerevisiae* cells after treatment with 750 µg mL^{-1} ZnONPs/SiO$_2$ for 6 h.

3.6. Effect of ZnONPs/ZnS on *S. cerevisiae* and *C. reinhardtii* cell viability

Figures 9A, 9B and 9C show the cytotoxic impact of various particle concentrations of ZnONPs/ZnS on the *C. reinhardtii* cell viability upon irradiation under visible and UV light or in dark conditions at various exposure times up to 6 h. We did not detect a measurable effect upon exposure to a series of different particle concentrations of ZnONPs/ZnS at 25 °C for up to 2 h as shown in Figure 9A and 9B. These findings were also indirectly confirmed by the SEM images of the treated *C. reinhardtii* cell samples (Figure 4E). The impact of ZnONPs/ZnS at particle concentrations 50-250 µg mL^{-1} on the *C. reinhardtii* cell viability illuminated with UV light for 6 h (Figure 9C) was higher than that in dark and under visible light. Figure 9D shows that the *S. cerevisiae* cells remain unaffected after 10 min of incubation in dark conditions which also agrees with the results obtained with *S. cerevisiae* irradiated with visible and UV light for the same period and particle concentration.

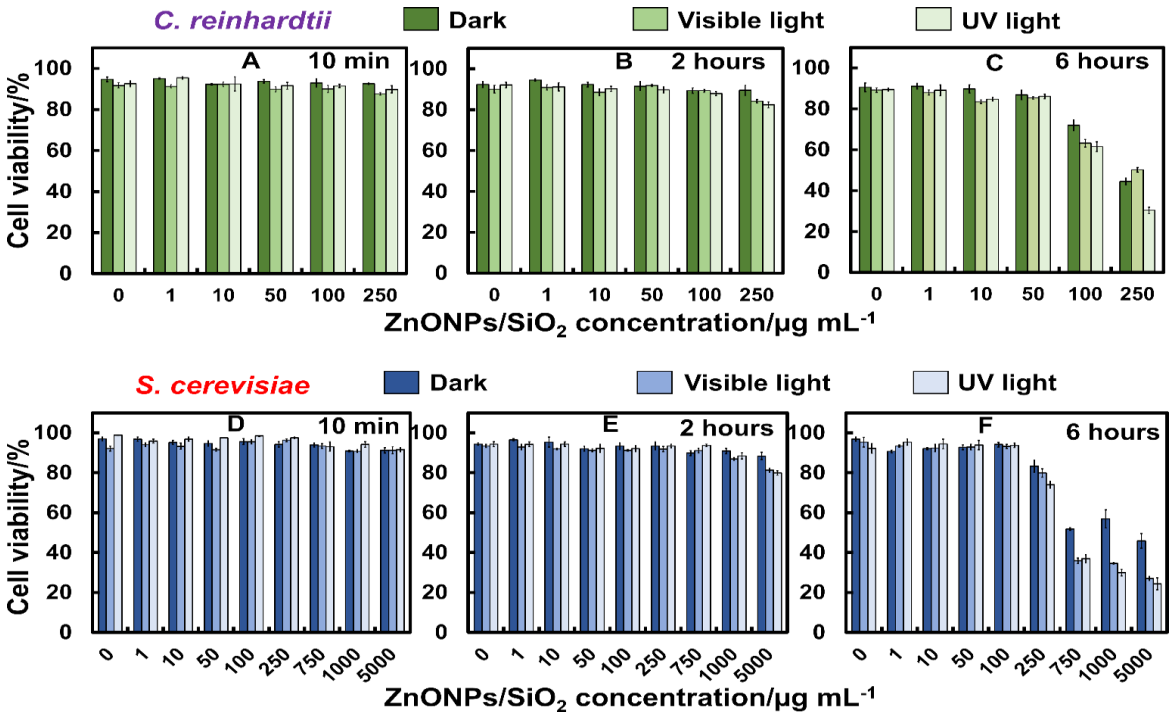

Figure 8. The effect of ZnONPs coated with a layer of silica on the viability of (A, B, C) *C. reinhardtii* and (D, E, F) *S. cerevisiae* cells at different particle concentrations. The data are presented as average ± SD (n = 3). The cells were incubated with the ZnONPs/SiO_2 at various exposure times in dark conditions, and under visible and UV light.

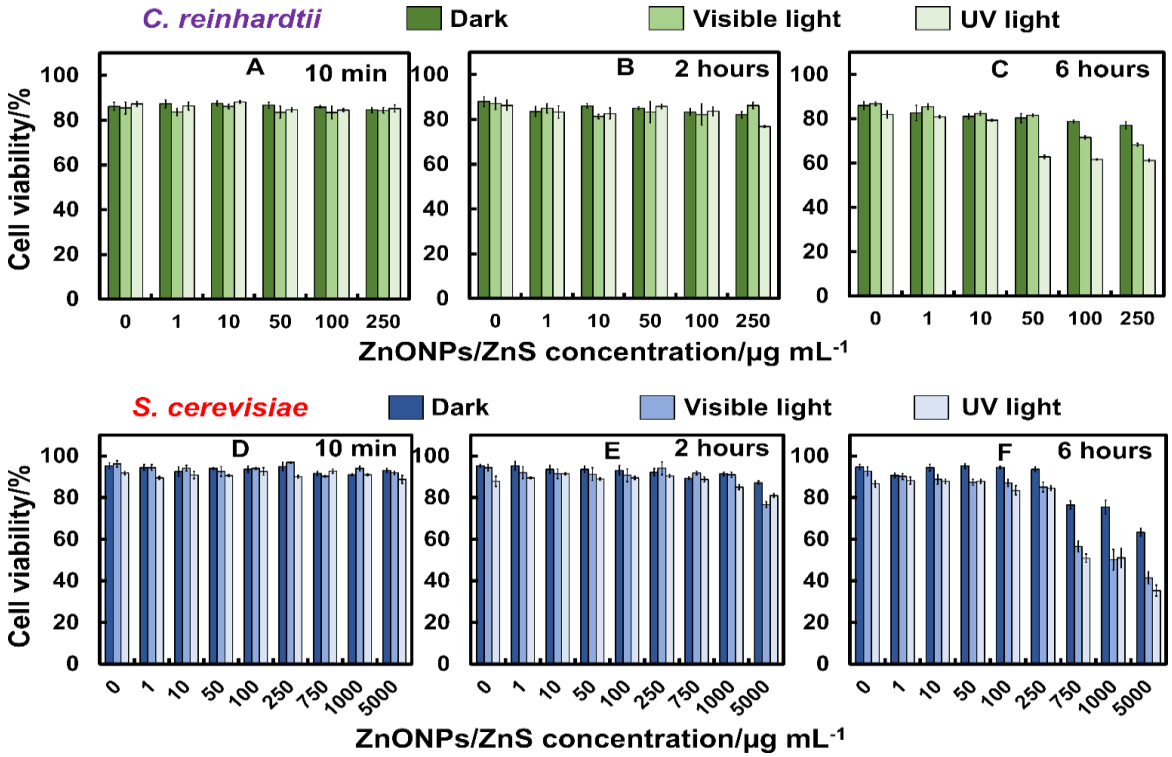

Figure 9. The effect of ZnONPs coated with a layer of ZnS on the viability of (A, B, C) *C. reinhardtii* and (D, E, F) *S. cerevisiae* cells at different particle concentrations. The cells were incubated with the ZnONPs/ZnS at various exposure times in dark conditions, and under visible and UV light, respectively.

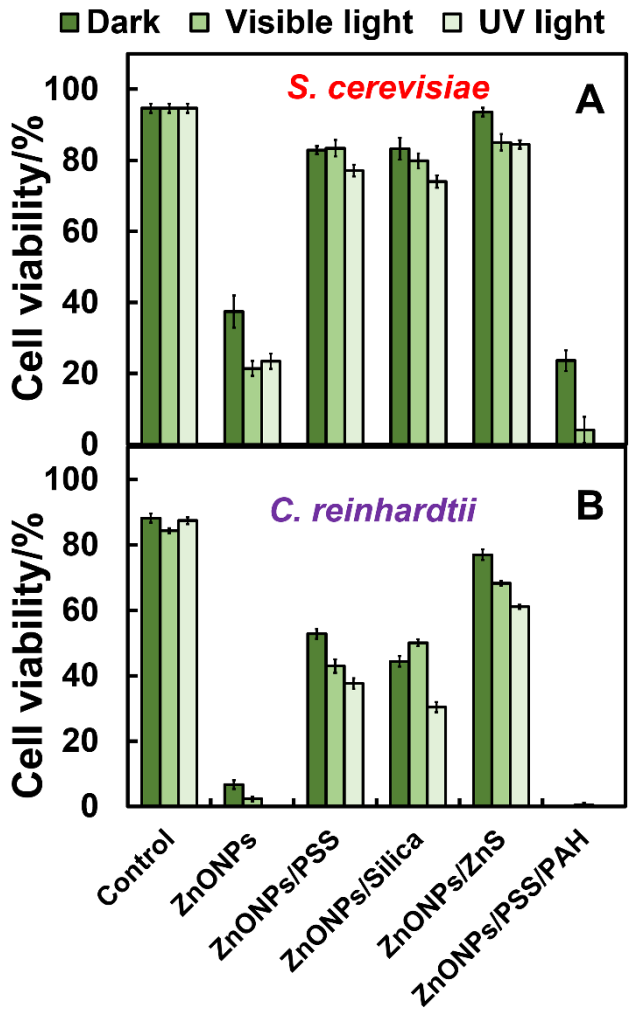

Figure 10. Comparison of the effect of bare ZnONPs, ZnONPs/PSS, ZnONPs/SiO_2, ZnONPs/ZnS and ZnONPs/PSS/PAH on the viability of (A) *S. cerevisiae* and (B) *C. reinhardtii* cells at particle concentration 250 µg mL^{-1}. The cells were treated with the nanoparticles in dark conditions, and under visible and UV light for 6 h, respectively.

After 2 h (Figure 9E) of incubation at higher concentration of ZnONPs/ZnS (5000 µg mL^{-1}), there was a very strong decrease in the *S. cerevisiae* cell viability, but the impact was smaller at lower concentrations both in dark condition, and under visible and UV light. After 6 h of exposure under visible and UV light, there was a considerable loss of the yeast cell viability for concentrations of ZnONPs/ZnS in the range of 750-5000 µg mL^{-1}. However, in dark conditions, there was a slight effect on the *S. cerevisiae* for ZnONPs/ZnS concentrations up to 5000 µg mL^{-1} (Figure 9F). Our tests showed that at 5000 µg mL^{-1} ZnONPs/ZnS under UV light, a significant impact occurred with about 30% loss of the cell viability in comparison with the control sample. This result may be explained by ROS released on the particle surface under UV light, which cause to the nearby cells. However, since these particles do not attach to the cells, a very high concentration of ZnONPs/ZnS is needed to produce even a weak toxic effect on the cells viability. This was confirmed by the both TEM and SEM images (Figure 6E and Figure 7E). Figure 10 summarizes the effect of bare ZnONPs, ZnONPs/PSS, ZnONPs/SiO_2, ZnONPs/ZnS and ZnONPs/PSS/PAH on *C. reinhardtii* and *S. cerevisiae* cell viability under the same conditions at particle concentration 250 µg mL^{-1} for 6 h. This result indicated that the bare ZnONPs and ZnONPs/PSS/PAH have a strong effect on the *C. reinhardtii* and *S. cerevisiae* cell viability at concentration above 250 µg mL^{-1} for 6 h both in dark conditions and under visible and UV light, respectively. Very similar effect was observed for ZnONPs/PSS, ZnONPs/SiO_2 and ZnONPs/ZnS on *S. cerevisiae* cells as shown in Figure 10A. These results show that the anti-yeast effect of the bare ZnONPs, ZnONPs/PSS, ZnONPs/SiO_2, ZnONPs/ZnS and ZnONPs/PSS/PAH is much smaller than that on *C. reinhardtii* (Figure 10B).

4. Conclusions

Here we explored and discussed the mechanisms by which such bare and surface modified ZnONPs attack algal and yeast cells, which involves ROS generation upon irradiation with UV light, as well as the potential dislocation of the cell membrane due to the ZnONPs cationic surface combined with its rough surface morphology, ROS scavenging, release of metal ions, as Zn^{2+} on the cell surface and the role of the nanoparticle attachment to the microbial cell walls. We studied various ways to impact the antimicrobial activity of a range of surface-treated ZnONPs on two types of microbial species: *C. reinhardtii* as a typical microalgae representative and *S. cerevisiae* as yeast. Our present work indicate that bare ZnONPs had significant toxicity impact against *C. reinhardtii* and *S. cerevisiae* cells and their impact increased upon increasing the ZnONPs concentration. The loss of algae cell viability was also accompanied with a decline in the chlorophyll content after up to 6 h of incubation with ZnONPs in dark conditions and upon illumination with visible and UV light. This showed that ZnONPs could not only damage the cell wall but also may degrade the cell chloroplasts by ROS generation. The results from TEM and SEM analysis of cell samples incubated with ZnONPs showed that the particles accumulate on the outer cell wall of both *S. cerevisiae* and *C. reinhardtii* which is very important for their effective anti-algal and anti-yeast action. In order to explore the effect of the surface coating, a series of ZnONPs coated with zinc sulfide, silica or polyelectrolytes were synthesized and their antimicrobial effect towards yeast and microalgae was compared to this of the non-coated ZnONPs. It was discovered that the anti-algal and anti-yeast activity of the surface-modified ZnONPs alternates with the particle surface charge. The nanoparticles of anionic surface (ZnONPs/ZnS, ZnONPs/SiO_2 and ZnONPs/PSS) had much lower anti-algal and anti-yeast activity than the ones of cationic surfaces (ZnONPs/PSS/PAH and bare ZnONPs). In general, bare ZnONPs and ZnONPs/PSS/PAH showed remarkable anti-yeast and anti-algal activity and demonstrated high efficiency against these microbial cells, even at low particle concentrations. Our results provide new insights about the effect of the ZnONPs surface coatings on their antimicrobial action and could potentially lead to development better anti-yeast and anti-algal formulations.

ACKNOWLEDGMENTS

A.F.H. thanks the Iraqi Government, the Higher Committee for Education Development of Iraq and the University of Babylon,

Iraq for the financial support for his PhD study during the work on this project. The authors appreciated the technical help from Tony Sinclair and Ann Lowry at the University of Hull Microscopy Suite with the SEM and TEM sample preparation and imaging.

ORCID

Ahmed F. Halbus: 0000-0001-9060-7073
Tommy S. Horozov: 0000-0001-8818-3750
Vesselin N. Paunov: 0000-0001-6878-1681

Author Contributions

VNP gave the idea for the study, supervised the project and provided technical advice. TSH co-supervised AFH and participated in the project discussions. VNP prepared some of the artwork. AFH did the experimental work and put together the draft manuscript which was then co-edited and completed through contributions of all authors. All authors have given approval to the final version of the manuscript.

FUNDING SOURCES

AFH acknowledge funding from the Higher Committee for Education Development of Iraq and the University of Babylon, Iraq for financial support of this study.

ASSOCIATED CONTENT

In the enclosed electronic supplementary information (ESI) we present the following additional data: (1) Time-Kill assay statistical analysis; (2) Preparation of polyelectrolyte-coated ZnONPs; (3) The effect of addition of ZnONPs to polyelectrolyte (PSS); (4) The zeta potential of polyelectrolyte (PSS) coated ZnONPs in dark conditions, under visible and UV lights; (5) The UV-Vis spectroscopy data and thermogravimetric analysis (TGA) of ZnONPs; (6) Calcination of the synthesized ZnONPs; (7) Energy dispersive X-ray diffractive (EDX) of ZnONPs; (8) EDX of ZnS coating of zinc oxide nanoparticles; (9) EDX of silica coating of zinc oxide nanoparticles by the Stöber process; (10) Polyelectrolyte coating of zinc oxide nanoparticles; (11) Determination of the chlorophyll content of microalgae cells; (12) Chlorophyll content of microalgae after exposure to ZnONPs; (13) Effect of the Zn^{2+} concentration on the *C. reinhardtii* viability.

References

(1) Rupasinghe, R. Dissolution and aggregation of zinc oxide nanoparticles at circumneutral pH; a study of size effects in the presence and absence of citric acid. **2011**.
(2) Zhang, J. In *Silver-coated zinc oxide nanoantibacterial synthesis and antibacterial activity characterization*, Electronics and Optoelectronics (ICEOE), 2011 International Conference on, IEEE: 2011; pp V3-94-V3-98.
(3) Hussein, F. H.; Halbus, A. F. Rapid decolorization of cobalamin. *International Journal of Photoenergy* **2012,** *2012*, 1-9.
(4) Nirmala, M.; Nair, M. G.; Rekha, K.; Anukaliani, A.; Samdarshi, S.; Nair, R. G. Photocatalytic activity of ZnO nanopowders synthesized by DC thermal plasma. *Afr J Basic Appl Sci* **2010,** *2*, 161-166.
(5) Sirelkhatim, A.; Mahmud, S.; Seeni, A.; Kaus, N. H. M.; Ann, L. C.; Bakhori, S. K. M.; Hasan, H.; Mohamad, D. Review on zinc oxide nanoparticles: antibacterial activity and toxicity mechanism. *Nano-Micro Letters* **2015,** *7* (3), 219-242.
(6) Zhang, H.; Chen, B.; Jiang, H.; Wang, C.; Wang, H.; Wang, X. A strategy for ZnO nanorod mediated multi-mode cancer treatment. *Biomaterials* **2011,** *32* (7), 1906-1914.
(7) Seil, J. T.; Taylor, E. N.; Webster, T. J. In *Reduced activity of Staphylococcus epidermidis in the presence of sonicated piezoelectric zinc oxide nanoparticles*, Bioengineering Conference, 2009 IEEE 35th Annual Northeast, IEEE: 2009; pp 1-2.
(8) Halbus, A. F.; Horozov, T. S.; Paunov, V. N. Colloid particle formulations for antimicrobial applications. *Advances in Colloid and Interface Science* **2017**, *249*, 134-148.
(9) Seven, O.; Dindar, B.; Aydemir, S.; Metin, D.; Ozinel, M.; Icli, S. Solar photocatalytic disinfection of a group of bacteria and fungi aqueous suspensions with TiO_2, ZnO and Sahara desert dust. *Journal of Photochemistry and Photobiology A: Chemistry* **2004,** *165* (1), 103-107.
(10) Nagarajan, P.; Rajagopalan, V. Enhanced bioactivity of ZnO nanoparticles—an antimicrobial study. *Science and Technology of Advanced Materials* **2008,** *9* (3), 035004.
(11) Ahmed, S.; Rasul, M.; Martens, W. N.; Brown, R.; Hashib, M. Heterogeneous photocatalytic degradation of phenols in wastewater: a review on current status and developments. *Desalination* **2010,** *261* (1), 3-18.
(12) Espitia, P. N. d. FF Soares, JS dos Reis Coimbra, NJ de Andrade, RS Cruz and EAA Medeiros. *Food Bioprocess Technol* **2012,** *5*, 1447.
(13) Zhang, Y.; Ram, M. K.; Stefanakos, E. K.; Goswami, D. Y. Synthesis, characterization, and applications of ZnO nanowires. *Journal of Nanomaterials* **2012,** *2012*, 20.
(14) Sawai, J.; Shoji, S.; Igarashi, H.; Hashimoto, A.; Kokugan, T.; Shimizu, M.; Kojima, H. Hydrogen peroxide as an antibacterial factor in zinc oxide powder slurry. *Journal of Fermentation and Bioengineering* **1998,** *86* (5), 521-522.
(15) Dunford, R.; Salinaro, A.; Cai, L.; Serpone, N.; Horikoshi, S.; Hidaka, H.; Knowland, J. Chemical oxidation and DNA damage catalysed by inorganic sunscreen ingredients. *FEBS letters* **1997,** *418* (1), 87-90.
(16) Reddy, K. M.; Feris, K.; Bell, J.; Wingett, D. G.; Hanley, C.; Punnoose, A. Selective toxicity of zinc oxide nanoparticles to prokaryotic and eukaryotic systems. *Applied physics letters* **2007,** *90* (21), 213902.
(17) Raghupathi, K. R.; Koodali, R. T.; Manna, A. C. Size-dependent bacterial growth inhibition and mechanism of antibacterial activity of zinc oxide nanoparticles. *Langmuir* **2011,** *27* (7), 4020-4028.
(18) Yamamoto, O. Influence of particle size on the antibacterial activity of zinc oxide. *International Journal of Inorganic Materials* **2001,** *3* (7), 643-646.
(19) Nair, S.; Sasidharan, A.; Rani, V. D.; Menon, D.; Nair, S.; Manzoor, K.; Raina, S. Role of size scale of ZnO nanoparticles and microparticles on toxicity toward bacteria and osteoblast cancer cells. *Journal of Materials Science: Materials in Medicine* **2009,** *20* (1), 235-241.
(20) Aruoja, V.; Dubourguier, H.-C.; Kasemets, K.; Kahru, A. Toxicity of nanoparticles of CuO, ZnO and TiO_2 to microalgae Pseudokirchneriella subcapitata. *Science of the total environment* **2009,** *407* (4), 1461-1468.
(21) Heinlaan, M.; Ivask, A.; Blinova, I.; Dubourguier, H.-C.; Kahru, A. Toxicity of nanosized and bulk ZnO, CuO and TiO_2 to bacteria Vibrio fischeri and crustaceans Daphnia magna and Thamnocephalus platyurus. *Chemosphere* **2008,** *71* (7), 1308-1316.
(22) Al-Awady, M. J.; Greenway, G. M.; Paunov, V. N. Nanotoxicity of polyelectrolyte-functionalized titania nanoparticles towards microalgae and yeast: role of the particle concentration, size and surface charge. *RSC Advances* **2015,** *5* (46), 37044-37059.
(23) Hu, C.; Li, M.; Cui, Y.; Li, D.; Chen, J.; Yang, L. Toxicological effects of TiO_2 and ZnO nanoparticles in soil on earthworm Eisenia fetida. *Soil Biology and Biochemistry* **2010,** *42* (4), 586-591.

(24) Kasemets, K.; Ivask, A.; Dubourguier, H.-C.; Kahru, A. Toxicity of nanoparticles of ZnO, CuO and TiO_2 to yeast Saccharomyces cerevisiae. *Toxicology in vitro* **2009,** *23* (6), 1116-1122.
(25) Hoshino, A.; Fujioka, K.; Oku, T.; Suga, M.; Sasaki, Y. F.; Ohta, T.; Yasuhara, M.; Suzuki, K.; Yamamoto, K. Physicochemical properties and cellular toxicity of nanocrystal quantum dots depend on their surface modification. *Nano Letters* **2004,** *4* (11), 2163-2169.
(26) Mudunkotuwa, I. A.; Grassian, V. H. Citric acid adsorption on TiO_2 nanoparticles in aqueous suspensions at acidic and circumneutral pH: surface coverage, surface speciation, and its impact on nanoparticle− nanoparticle interactions. *Journal of the American Chemical Society* **2010,** *132* (42), 14986-14994.
(27) Ghorbani, H. R.; Mehr, F. P.; Pazoki, H.; Rahmani, B. M. Synthesis of ZnO Nanoparticles by Precipitation Method. *Oriental Journal of Chemistry* **2015,** *31* (2), 1219-1221.
(28) Sadollahkhani, A.; Kazeminezhad, I.; Lu, J.; Nur, O.; Hultman, L.; Willander, M. Synthesis, structural characterization and photocatalytic application of ZnO@ ZnS core–shell nanoparticles. *RSC Advances* **2014,** *4* (70), 36940-36950.
(29) Stöber, W.; Fink, A.; Bohn, E. Controlled growth of monodisperse silica spheres in the micron size range. *Journal of colloid and interface science* **1968,** *26* (1), 62-69.
(30) Tadanaga, K.; Morita, K.; Mori, K.; Tatsumisago, M. Synthesis of monodispersed silica nanoparticles with high concentration by the Stöber process. *J. Sol-gel sci. and technol.* **2013,** *68* (2), 341-345.
(31) Wang, H. *Development of silica based nanopigments*; Lehrstuhl für Textilchemie und Makromolekulare Chemie: 2013.
(32) Halbus, A. F.; Horozov, T. S.; Paunov, V. N. Strongly Enhanced Antibacterial Action of Copper Oxide Nanoparticles with Boronic Acid Surface Functionality. *ACS applied materials & interfaces* **2019**. *11*, 12232–12243.
(33) Al-Obaidy, S. S. M.; Halbus, A. F.; Greenway, G. M.; Paunov, V. N. Boosting the antimicrobial action of vancomycin formulated in shellac nanoparticles of dual-surface functionality. *Journal of Materials Chemistry B* **2019**, DOI: 10.1039/C8TB03102A.
(34) Yu, J.; Yu, X. Hydrothermal synthesis and photocatalytic activity of zinc oxide hollow spheres. *Environmental science & technology* **2008,** *42* (13), 4902-4907.
(35) Hoffmann, M. R.; Martin, S. T.; Choi, W.; Bahnemann, D. W. Environmental applications of semiconductor photocatalysis. *Chemical reviews* **1995,** *95* (1), 69-96.
(36) Bagheri, S.; Chandrappa, K.; Hamid, S. B. A. Facile synthesis of nano-sized ZnO by direct precipitation method. *Der Pharma Chemica* **2013,** *5* (3), 265-270.
(37) Bagabas, A.; Alshammari, A.; Aboud, M. F.; Kosslick, H. Room-temperature synthesis of zinc oxide nanoparticles in different media and their application in cyanide photodegradation. *Nanoscale research letters* **2013,** *8* (1), 1.
(38) Raoufi, D. Synthesis and microstructural properties of ZnO nanoparticles prepared by precipitation method. *Renewable Energy* **2013,** *50*, 932-937.
(39) Salahuddin, N. A.; El-Kemary, M.; Ibrahim, E. M. Synthesis and Characterization of ZnO Nanoparticles via Precipitation Method: Effect of Annealing Temperature on Particle Size. *Nanoscience and Nanotechnology* **2015,** *5* (4), 82-88.
(40) Ye, J.; Zhou, R.; Zheng, C.; Sun, Q.; Lv, Y.; Li, C.; Hou, X. Size-controllable synthesis of spherical ZnO nanoparticles: Size-and concentration-dependent resonant light scattering. *Microchemical Journal* **2012,** *100*, 61-65.
(41) Wang, Y.; Zhang, C.; Bi, S.; Luo, G. Preparation of ZnO nanoparticles using the direct precipitation method in a membrane dispersion micro-structured reactor. *Powder Technology* **2010,** *202* (1), 130-136.
(42) Thirumavalavan, M.; Huang, K.-L.; Lee, J.-F. Preparation and morphology studies of nano zinc oxide obtained using native and modified chitosans. *Materials* **2013,** *6* (9), 4198-4212.
(43) Nagarajan, S.; Kuppusamy, K. A. Extracellular synthesis of zinc oxide nanoparticle using seaweeds of gulf of Mannar, India. *Journal of nanobiotechnology* **2013,** *11* (1), 1.
(44) Raj, L.; Jayalakshmy, E. Biosynthesis and characterization of zinc oxide nanoparticles using root extract of Zingiber officinale. *Orient J Chem* **2015,** *31*, 51-6.
(45) Ramasamy, M.; Kim, Y. J.; Gao, H.; Yi, D. K.; An, J. H. Synthesis of silica coated zinc oxide–poly (ethylene-co-acrylic acid) matrix and its UV shielding evaluation. *Materials Research Bulletin* **2014,** *51*, 85-91.
(46) Roselli, M.; Finamore, A.; Garaguso, I.; Britti, M. S.; Mengheri, E. Zinc oxide protects cultured enterocytes from the damage induced by Escherichia coli. *The Journal of Nutrition* **2003,** *133* (12), 4077-4082.
(47) Wahab, R.; Mishra, A.; Yun, S.-I.; Kim, Y.-S.; Shin, H.-S. Antibacterial activity of ZnO nanoparticles prepared via non-hydrolytic solution route. *Appl. microbiology & biotechnol.* **2010,** *87* (5), 1917-1925.
(48) Adams, L. K.; Lyon, D. Y.; Alvarez, P. J. Comparative eco-toxicity of nanoscale TiO_2, SiO_2, and ZnO water suspensions. *Water Res.* **2006,** *40* (19), 3527-3532.
(49) Hirota, K.; Sugimoto, M.; Kato, M.; Tsukagoshi, K.; Tanigawa, T.; Sugimoto, H. Preparation of zinc oxide ceramics with a sustainable antibacterial activity under dark conditions. *Ceramics Intern.* **2010,** *36* (2), 497-506.
(50) Zhang, L.; Jiang, Y.; Ding, Y.; Povey, M.; York, D. Investigation into the antibacterial behaviour of suspensions of ZnO nanoparticles (ZnO nanofluids). *J. Nanoparticle Res.* **2007,** *9* (3), 479-489.
(51) Halbus, A. F.; Horozov, T. S.; Paunov, V. N. Self-Grafting Copper Oxide Nanoparticles Show a Strong Enhancement of Their Anti-Algal and Anti-Yeast Action. *Nanoscale Adv.* **2019**, *1*, 2323-2336.
(52) Halbus, A. F.; Horozov, T. S.; Paunov, V. N. "Ghost" Silica Nanoparticles of "Host"-Inherited Antibacterial Action. *ACS Applied Materials and Interfaces* **2019**, *11*, 38519−38530.

TOC graphics